ISTITUTO NAZIONALE DI FISICA NUCLEARE

Sezione di Milano

INFN/TC-83/9
22 Aprile 1983

E. Fabrici and A. Salomone: ACCELERATION STUDIES FOR THE MILAN SUPERCONDUCTING CYCLOTRON

Servizio Documentazione
dei Laboratori Nazionali di Frascati

Istituto Nazionale di Fisica Nucleare
Sezione di Milano

INFN/TC-83/9
22 Aprile 1983

ACCELERATION STUDIES FOR THE MILAN SUPERCONDUCTING CYCLOTRON

E. Fabrici and A. Salomone
University of Milan, and INFN, Sezione di Milano

1. - INTRODUCTION

This paper present the results of an extensive analysis of the internal beam dynamics for the Milan superconducting cyclotron.

The aim of this work is to establish the conditions under which a sufficient beam to beam separation can be achieved at the extraction radius while preserving the accelerated beam quality in phase space.

As customary in cyclotrons, the method is to excite the $\nu_r = 1$ resonance with a first harmonic field component.

Since our cyclotron will accelerate a number of ions over a wide range of energies, beam dynamics studies have been carried out on a set of twelve ions representative of the entire operating range. This both in terms of the charge to mass ratio and of the magnetic field level.

The feasibility of accelerating $^3He^{++}$ has also been explored.

This study differs from the previous one, reported in ref. (1), mostly because of the different field maps used in the computations. As apparent in the following, only field maps pertaining to the final iron configuration have been used. The results thus obtained are deemed sufficiently consistent and reassuring, so that no further analysis will be carried out until magnetic field measurements are available.

2. - GENERAL CONSIDERATIONS

The features of the Milan superconducting cyclotron are extensively reported in ref. (2). Here we just recall the main characteristics of the extraction system, which is presented in Fig. 1.

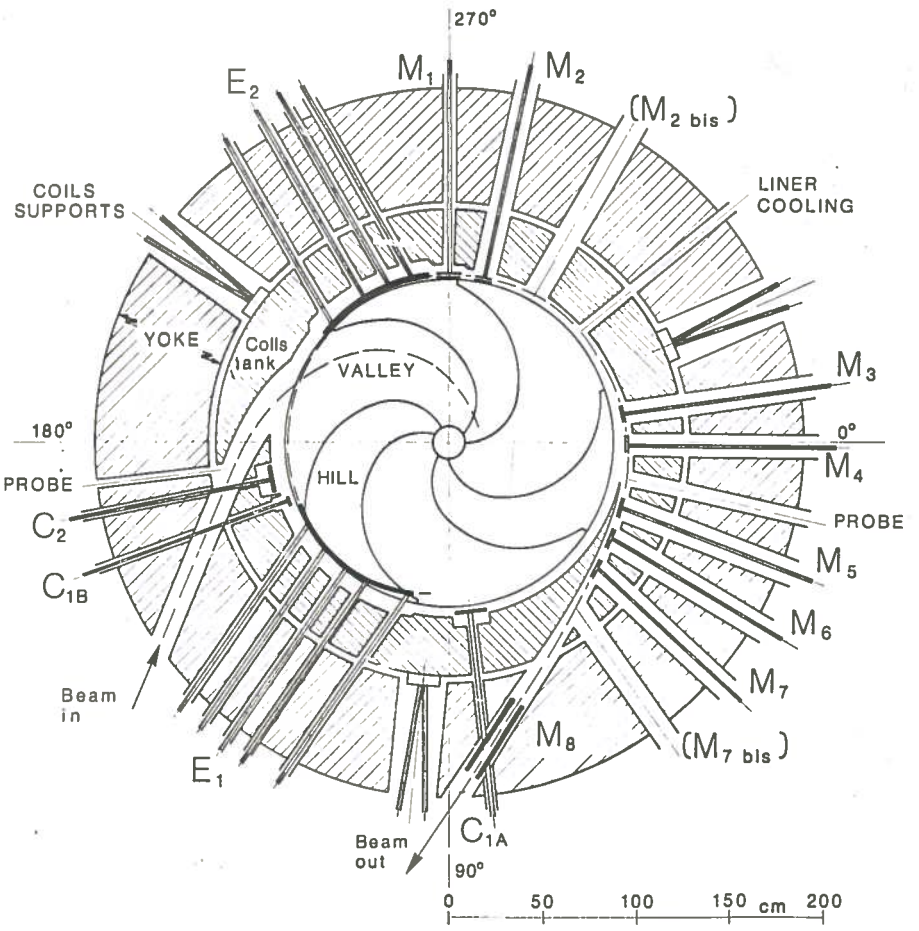

FIG. 1 - Median plane sketch showing the extraction system.

It consists of two electrostatic deflectors spanning an azimuthal range of 52 deg and 40 deg respectively, followed by seven passive magnetic channels. Another channel will be positioned in the yoke. For this one, however, it is still undecided whether it will be also passive or active, i. e. with some type of coil.

Also part of the extraction system are the iron bars C_{1A}, C_{1B} and C_2 that compensate for the first harmonic field perturbation produced by the iron channels. The first two, C_{1A} and C_{1B}, compensate the first two magnetic channels, M_1 and M_2, which are closest to the accelerated orbits. The overall effect produced by the other five M_3 to M_7, which are considerably farther out radially, can be compensated by a single bar, namely C_2.

A detailed discussion of the characteristics and performances of the extraction system is found in ref. (3).

The cyclotron operating diagram is shown in Fig. 2 in the $(Z/A, B_o)$ plane, B_o being the central field and Z/A the charge to mass ratio of the ions. The diagram is defined by the bending limit $K = 800$ (maximum kinetic energy equal to $K(Z/A)^2$), the focusing limit $K_{FOC} = 200$ (maximum kinetic energy equal to $K_{FOC}(Z/A)$), the line $Z/A = 0.5$ and the $B_o = 22$ kG limit[2].

The ions energy as a function of the rf frequency is plotted in Fig. 3 for various harmonic modes.

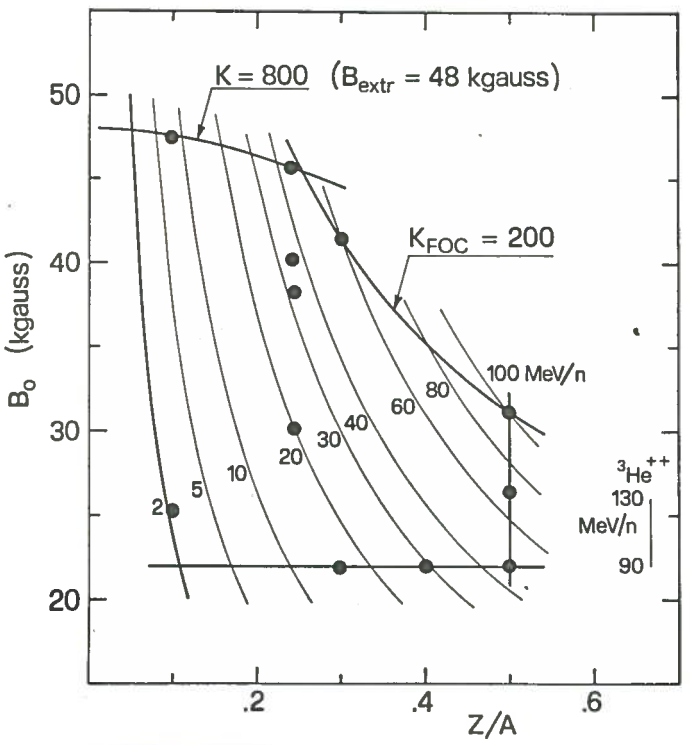

FIG. 2 - Operating diagram in the $(Z/A, B_o)$ plane. Constant T/A lines are also shown. Dots indicate representative ions for this study.

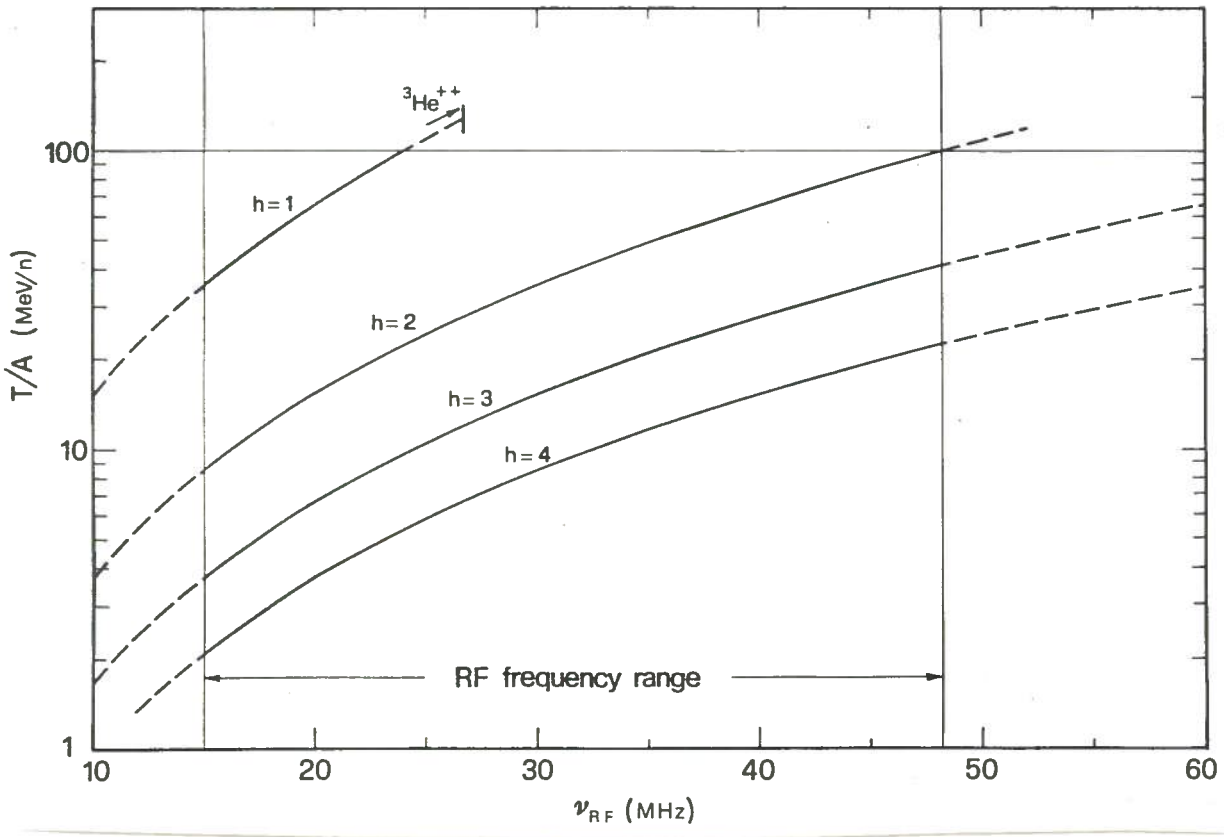

FIG. 3 - Energy per nucleon at extraction as a function of the rf frequency.

As already mentioned, twelve ions have been used to investigate the dynamic features of the machine. These ions, also listed in Table I, corresponds to the dots in the $(Z/A, B_o)$ diagram of Fig. 2 and are identified by their $Z/A/B_o$ numbers.

TABLE I - Charge to mass ratio central field levels and energy per nucleon after extraction for the twelve studied ions.

Z/A	B_o(kG)	T/A_F(MeV/n)
0.5	31.3	100.42
0.5	26.5	67.12
0.5	22	43.92
0.4	22	27.48
0.3	41.4	59.57
0.3	22	15.04
0.25	45.5	49.37
0.25	40	37.11
0.25	38	33.26
0.25	30	20.22
0.1	47.5	8.01
0.1	25	2.12

The eight ions on the limits of the operating diagram define the extreme running conditions of the machine, while the other four allow to check the regularity of the beam behaviour at intermediate conditions.

The process of determining the proper accelerating conditions in order to get the required beam to beam separation at extraction, while preserving the beam quality in phase space, is obviously an iterative one. However only the final results will be presented here.

First for each ion equilibrium orbit properties have been investigated. This has been carried out via an equilibrium orbit code using field maps with 120 deg symmetry. All maps are computed with an azimuthal step of 1 deg, a radial step of 1 cm, and according to the final coils and pole tip geometry as described in detail in ref. (4). Here we briefly recall that :

i) The average field produced by the iron is computed as a function of the coils excitation via the bidimensional magnetostatic code POISCR[5].

ii) The field produced by elements without cylindrical symmetry such as the center plug, hills, valleys etc. is computed as a function of radius and azimuth in the hypothesis of full saturation.

iii) The total average field is isochronized with a least square fitting procedure. The latter uses both the main coils and trim coils and takes into account, as a function of the coils excitation, the variations in the field produced by the iron.

Accelerated beam properties have been studied via the SPIRAL GAP code[6] on 360 deg maps which include the perturbing effects of the magnetic channels and compensating bars.

To provide realistic 360 deg maps, the magnetic field produced by the iron channels and compensating bars is required. This is computed as a function of azimuth and radius, in the hypothesis of full saturation, for the channels plus bars configuration required by every ion of Table I. The uncompensated first harmonic C_1 and second

harmonic C_2, produced by the magnetic channels, are plotted in Fig. 4 together with the compensated ones, for the ions with $Z/A = 0.5$ and central field values of 31.3 kG and 22 kG.

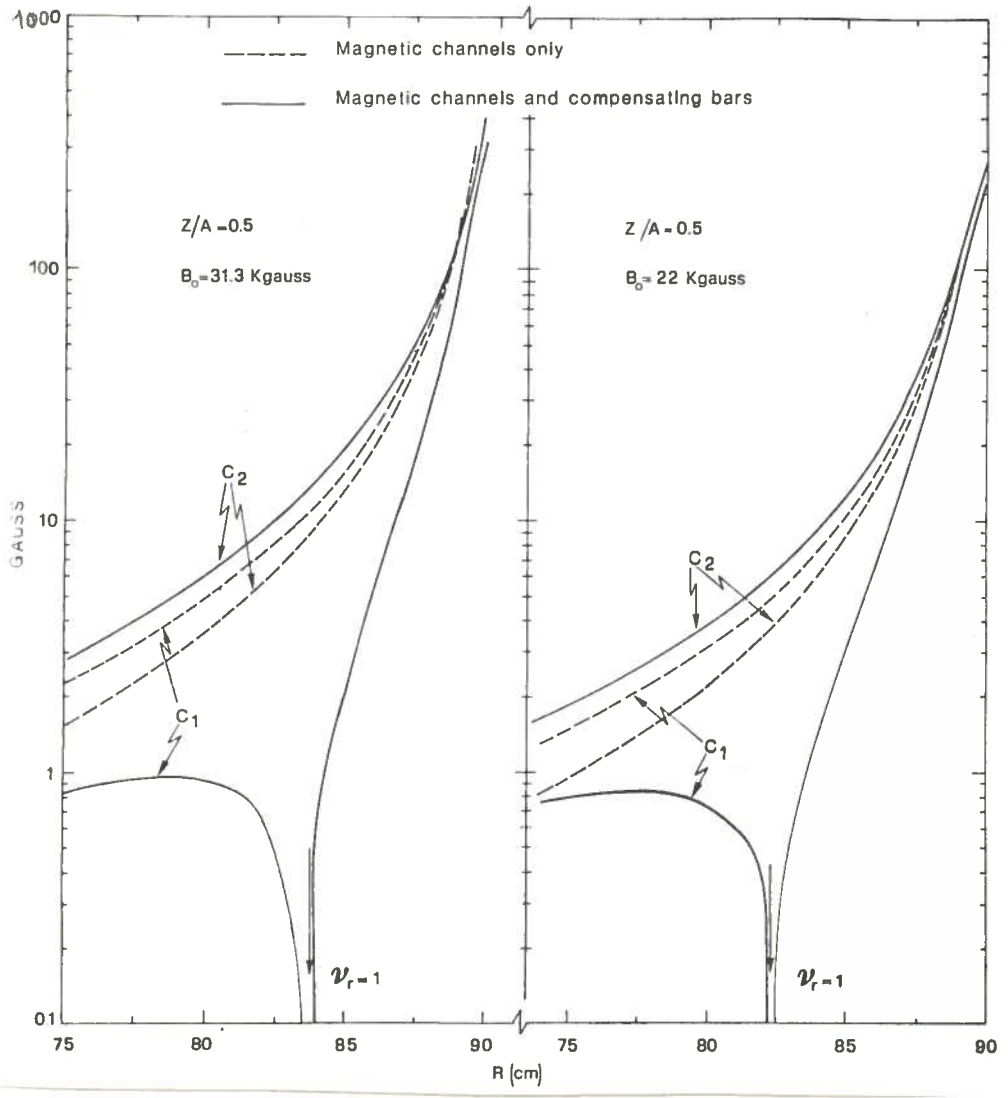

FIG. 4 - 1st and 2nd harmonics produced by the channels and compensating bars needed for extraction of the ions with $Z/A = 0.5$.

The compensated average field thus produced is also included in the fitting procedure. One such field, namely that produced by the channels plus bars configuration for the ion with $Z/A = 0.5$ and $B_o = 31.1$ kG, is shown in Fig. 5.

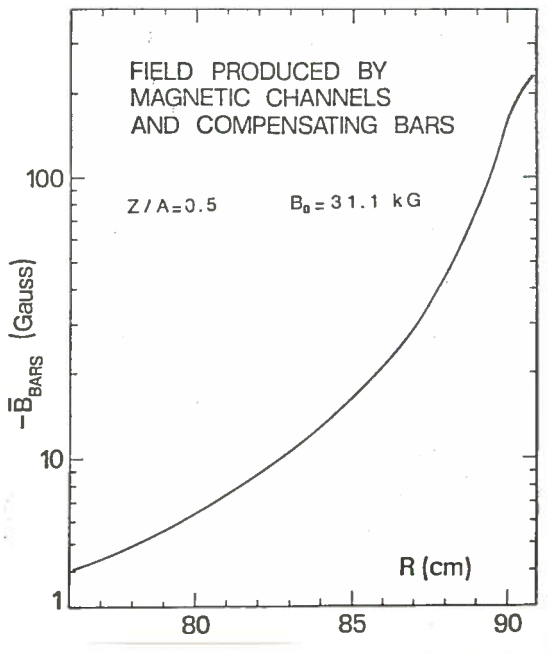

FIG. 5 - Average field produced by the magnetic channels plus compensating bars configuration required by the ion with $Z/A = 0.5$ and $B_o = 31.1$ kG.

This field has been actually used in the fitting procedure at all field levels because the differences in the average field produced by the channels plus bars configurations needed by the different ions are confined to a few gauss.

The need of including this field in the fitting procedure is evident in Fig. 6 where the beam phase as a function of energy is plotted for the ion with $Z/A = 0.5$ and $B_o = 31.1$ kG. The solid curve corresponds to the acceleration in a perfectly 120 deg symmetric field. The dotted one comes from acceleration in a field where $\overline{B}$ has been added after the isochronizing procedure. In the latter case larger phases at the extraction radius are obtained, reflecting a sensible non isochronism of the field thus produced.

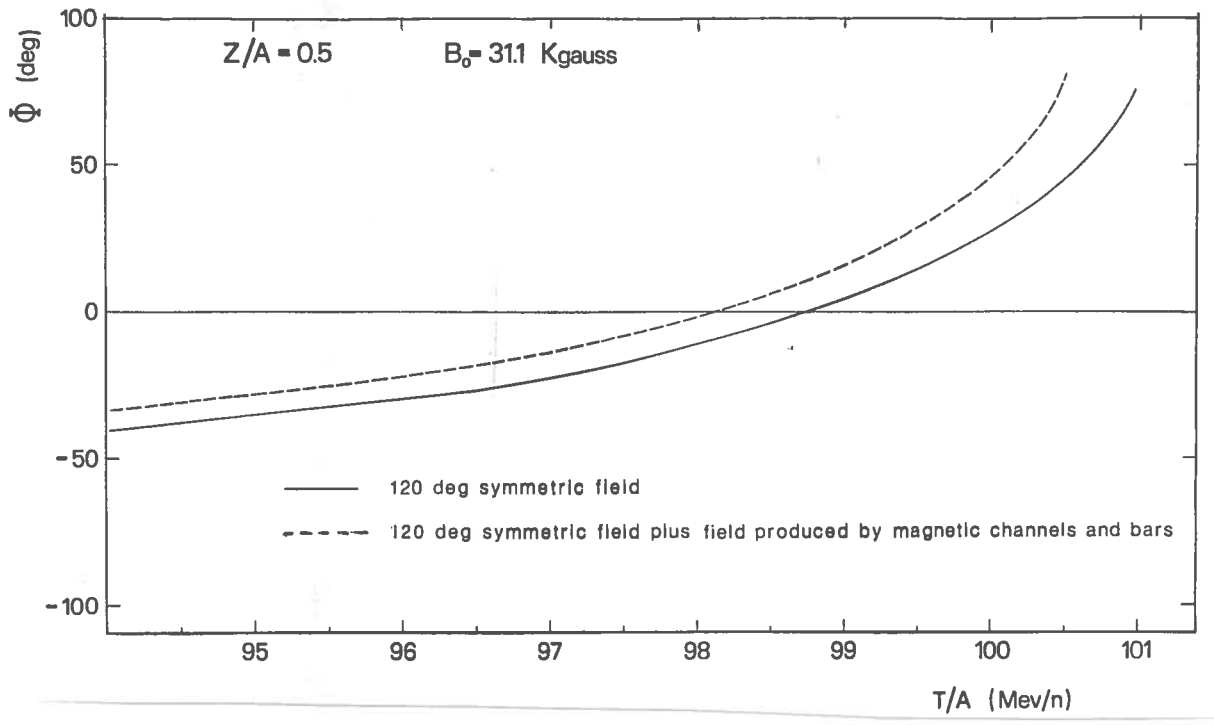

FIG. 6 - Beam phase with respect to the rf plotted as a function of the energy for the ion with $Z/A = 0.5$ and $B_o = 31.1$ kG. The lower curve correspond to a perfectly 120 deg symmetric field. The upper one comes from acceleration in a field where $\overline{B}$ has been added after the isochronizing procedure.

To obtain the 360 deg maps for acceleration studies the $\overline{B}$ contribution from channels and bars used in the fitting is subtracted from the 120 deg maps. Thereafter the 360 deg field map produced by the channels plus compensating bars configuration is added.

As stated above, a first harmonic field component is used in proximity of the $\nu_r = 1$ resonance to excite the radial precession and therefore to maximize the turn to turn separation at the deflector entry. The adjustment of the amplitude and phase of the first harmonic will be achieved through the 19th and 20th trim coils. They are wrapped around each hill and the independent excitation of the three sections

allows the control of the first harmonic amplitude and its phase.

An example of the first harmonic form factor produced by a combination of the 19th and 20th trim coils with opposite currents is shown in Fig. 7. However calculations presented in the following use a flat first harmonic form factor, which is eas-

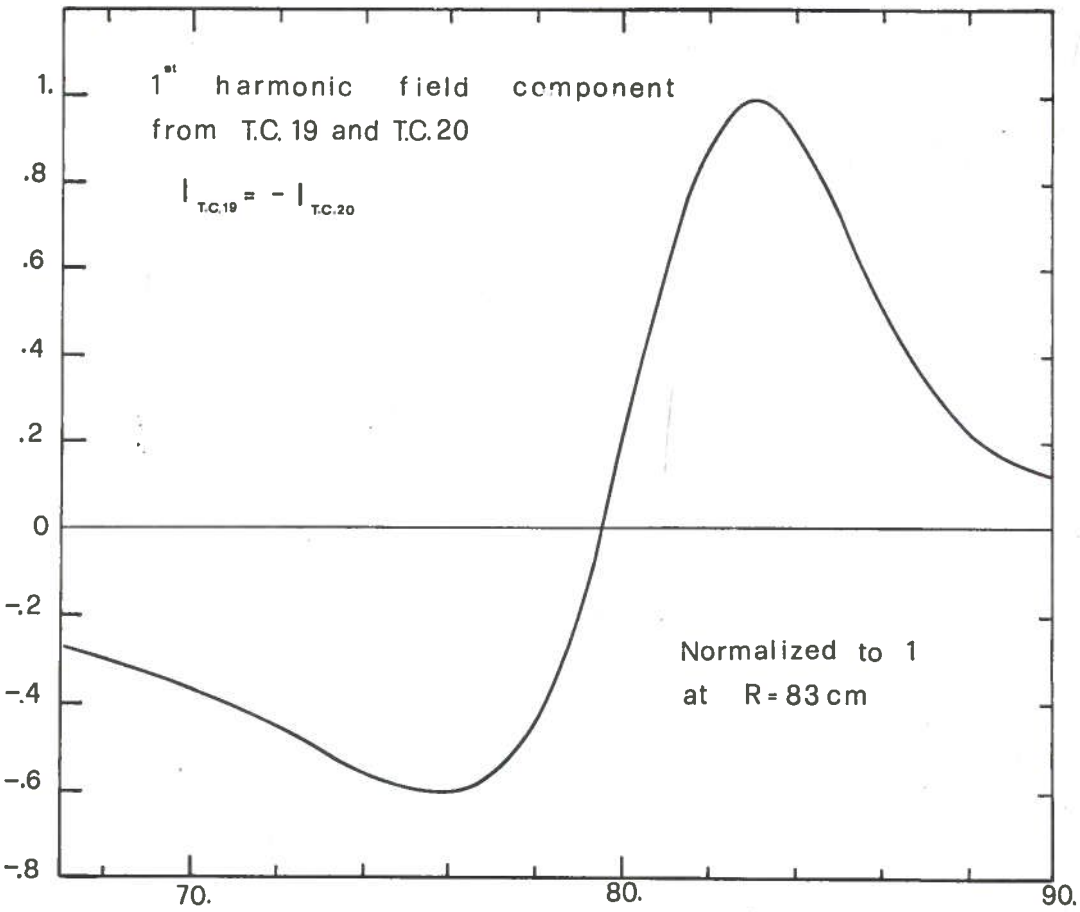

FIG. 7 - Form factor of the 1st harmonic produced by the 19th and 20th trim coil, for opposite currents in the two.

ier to handle. In this respect several tests performed on the most critical ion i. e. the one with $Z/A = 0.5$ and $B_o = 31.3$ kG have shown that there is no appreciable difference if the form factor of Fig. 7 is used in the computations. Physically this can be easily understood since what really matters is the first harmonic amplitude at the resonance, and therefore the details of the form factor at radii other than that of the resonance have little effect on the overall beam motion.

3. - EQUILIBRIUM ORBIT PROPERTIES

Equilibrium orbit properties like the average radius, $\bar{R}_{EO}$, the radial and axial focusing frequencies, ν_r, ν_z, and the phase, Φ, have been computed for the ions of Table I at a number of energies using a code performing Runge-Kutta integration with

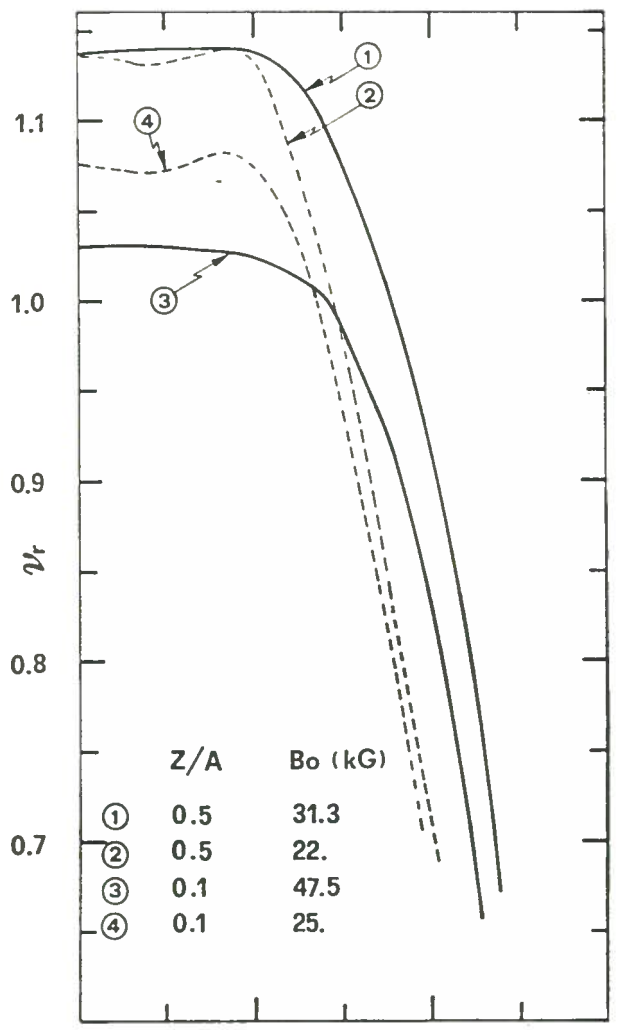

FIG. 8 - ν_r as a function of the average equilibrium orbit radius for four of the studied ions.

an azimuthal step of 2 deg.

The behaviour of ν_r near the extraction is of key importance for the design of the extraction system, and for four ions it is plotted as a function of the equilibrium orbit radius in Fig. 8.

It can be seen that any given ν_r value occurs at different radii depending upon the type of particle and field level. For example for $\nu_r = 0.76$, which corresponds to the minimum extractable energy for the ion with $Z/A = 0.5$ and $B_o = 31.3$ kG, the total radial span is about 2.5 cm. The curves of Fig. 8 show that at a fixed radius the range of ν_r is rather large. For example at 85 cm, ν_r varies from 0.65 to 0.92. These features have some consequences on the machine operation, like:

i) The radial span of the $\nu_r = 1$ resonance dictates the use of both the 19th and 20th trim coils to produce the first harmonic at the resonance, as anticipated in Par. 2.

ii) The extraction radius cannot be held constant and therefore a radially moveable extraction system has to be built.

Similar features are observed for the $\nu_r = 1$, $\nu_r = 2\nu_z$ and $\nu_r + 2\nu_z = 3$ resonances, whose positions have been located for all ions of Table I. The values of the average radius and energy corresponding to the crossing of these resonances are listed in Table II. The most pronounced effect is the shifting of the resonances radius, for a fixed ion, as a function of the field level. For the sake of example this is visualized in Fig. 9 for the ion with $Z/A = 0.25$.

Overall, the beam dynamics with respect to the resonances is best presented in the customary (ν_r, ν_z) plots. These are shown in Figg. 10 through 13 for the ions with, respectively, $Z/A = 0.5$, 0.25, 0.1 and $^3He^{++}$. Two or more field levels are considered for each ion, spanning the entire anticipated range.

The following features emerge from an examination of these figures:

TABLE II - Average equilibrium orbit radius and energy at which the different ions cross the resonances.

Z/A	B_o (kG)	$\nu_r = 2\nu_z$		$\nu_r = 1$		$\nu_r + 2\nu_z = 3$	
		$\overline{R}_{EO}$ (cm)	T/A_{EO} (MeV/n)	$\overline{R}_{EO}$ (cm)	T/A_{EO} (MeV/n)	$\overline{R}_{EO}$ (cm)	T/A_{EO} (MeV/n)
0.5	31.3	83.7	95.7	83.9	96.0	87.0	100.9
0.5	26.5	81.9	63.1	83.0	64.2	85.7	67.7
0.5	22	55.7	18.9	82.3	42.2	84.3	44.0
0.4	22	52.4	10.7	82.0	26.4	83.9	27.3
0.3	41.4	84.0	57.3	83.1	56.1	(*)	(*)
0.3	22	50.1	5.4	81.8	14.5	83.7	15.0
0.25	45.5	83.7	47.1	83.1	46.4	(*)	(*)
0.25	40	83.6	35.7	83.0	35.2	(*)	(*)
0.25	38	83.3	31.8	82.8	31.5	(*)	(*)
0.25	30	81.1	18.5	82.3	19.1	85.7	20.2
0.1	47.5	83.2	7.6	82.0	7.4	(*)	(*)
0.1	25	57.3	1.0	81.8	2.0	84.7	2.1

(*) The resonance is not observed before extraction.

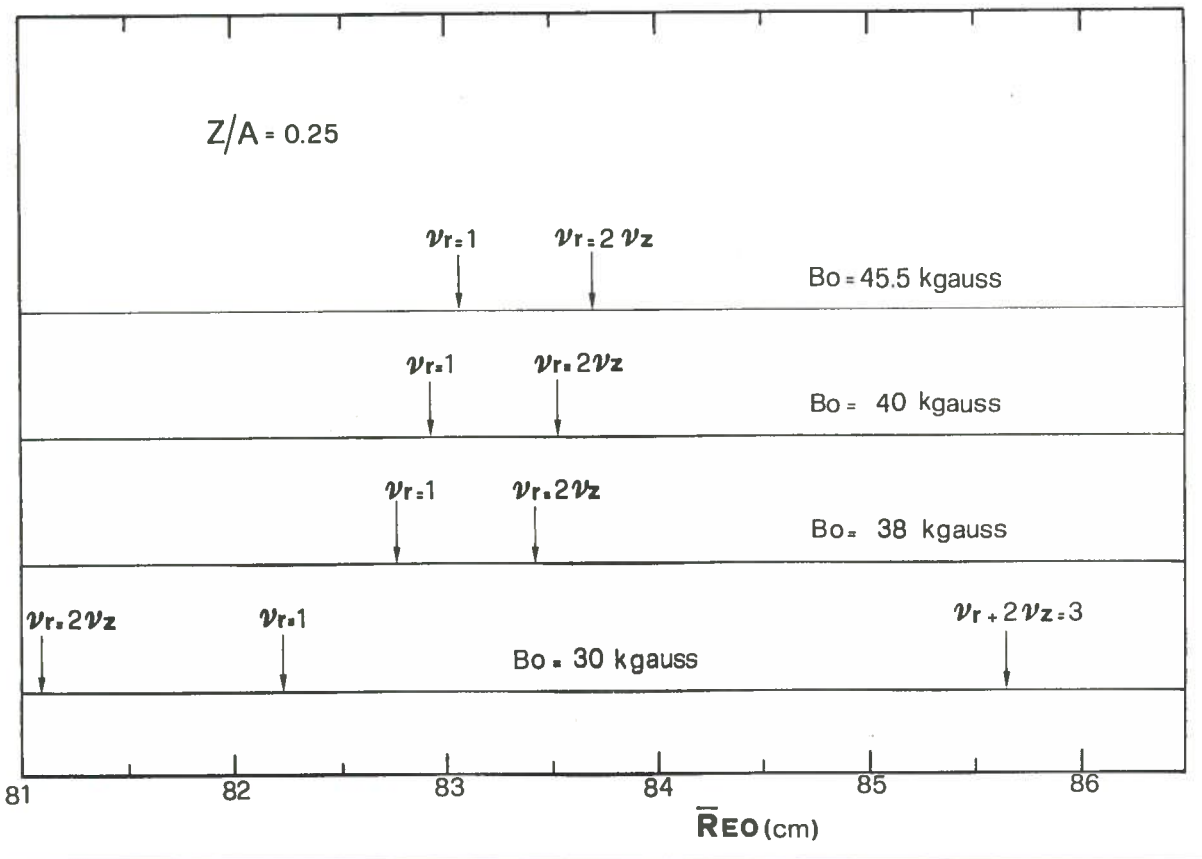

FIG. 9 - Resonances positions as a function of the average equilibrium orbit radius for the ion with Z/A = 0.25 at different field levels.

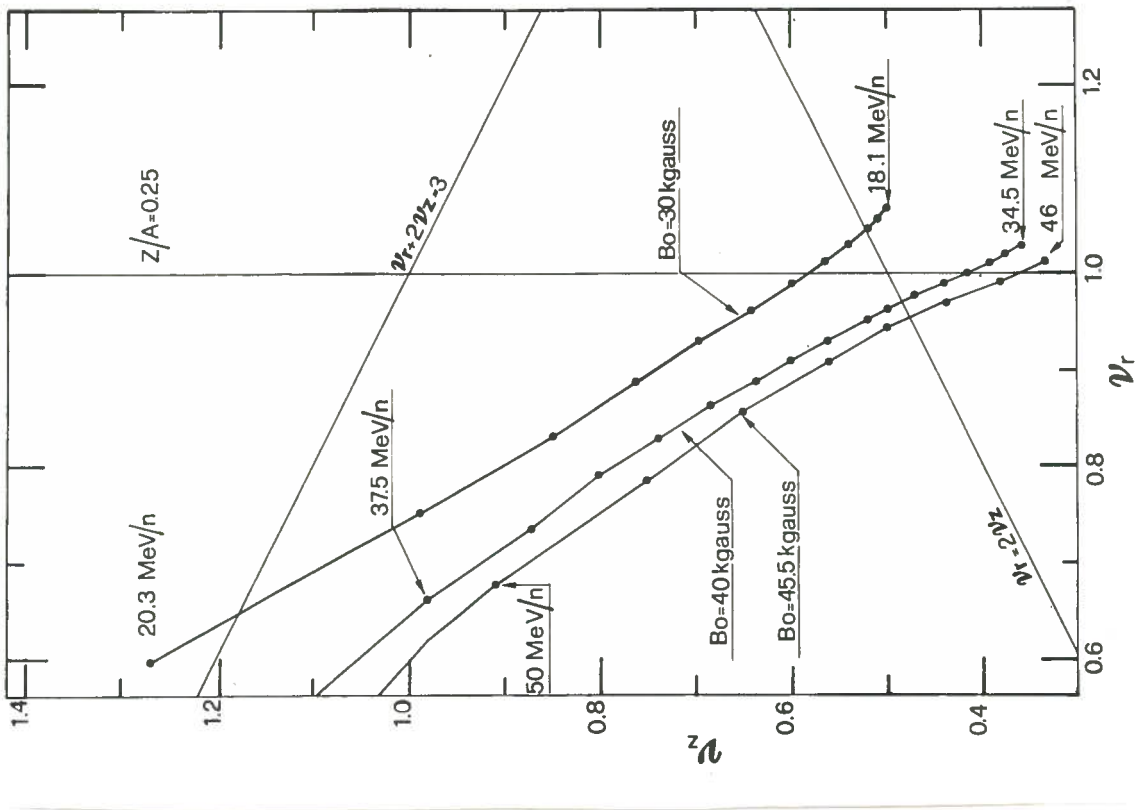

FIG. 11 - Operating (ν_r, ν_z) plots for the ion with $Z/A = 0.25$ at different field levels.

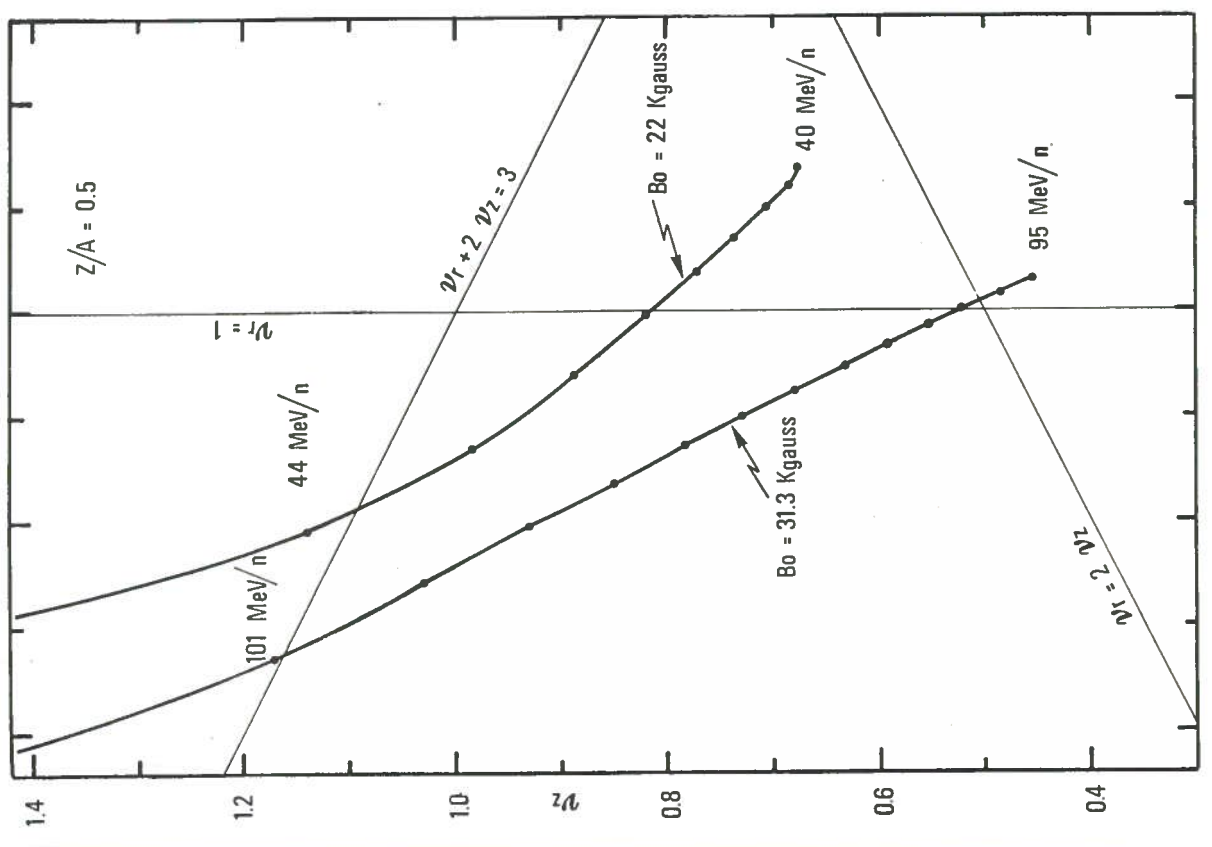

FIG. 10 - Operating (ν_r, ν_z) plots for the ion with $Z/A = 0.5$ at different field levels.

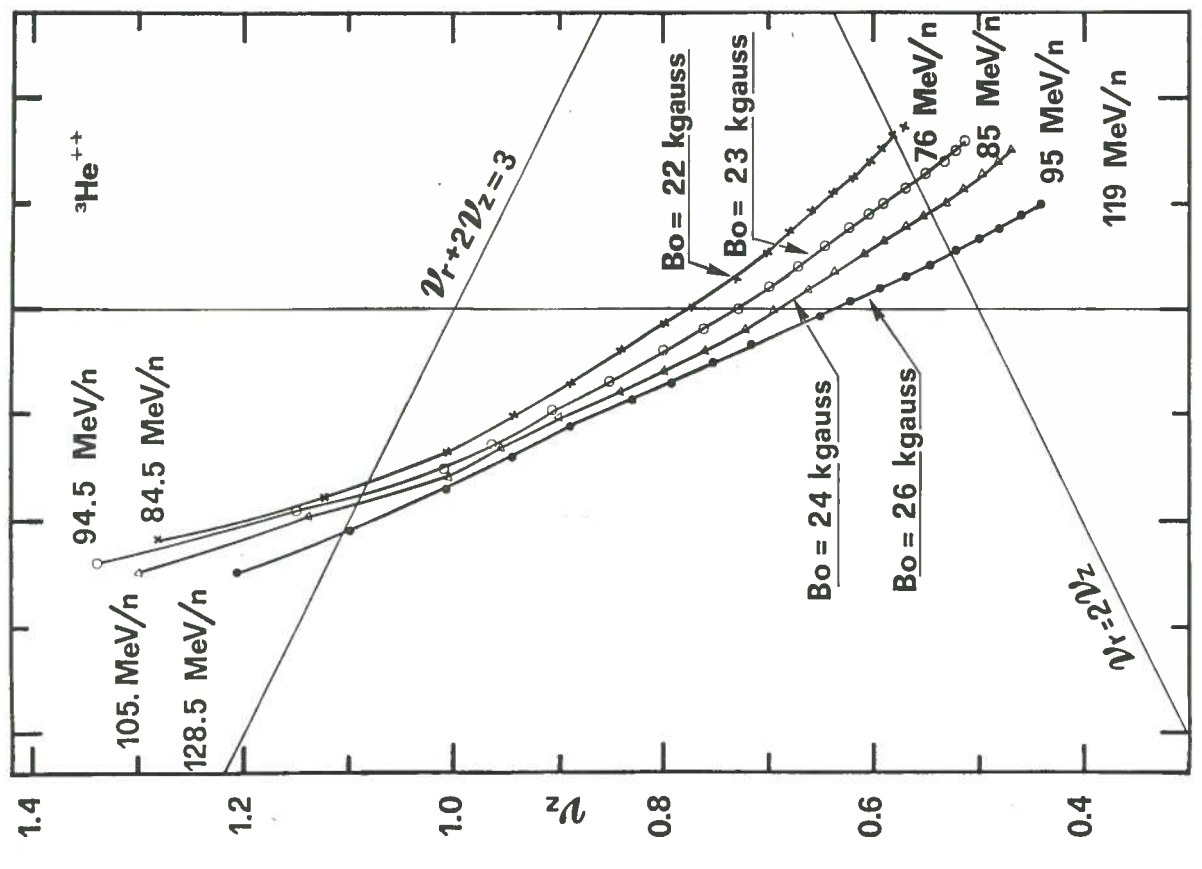

FIG. 13 - Operating (ν_r, ν_z) plots for $^3He^{++}$ at different field levels.

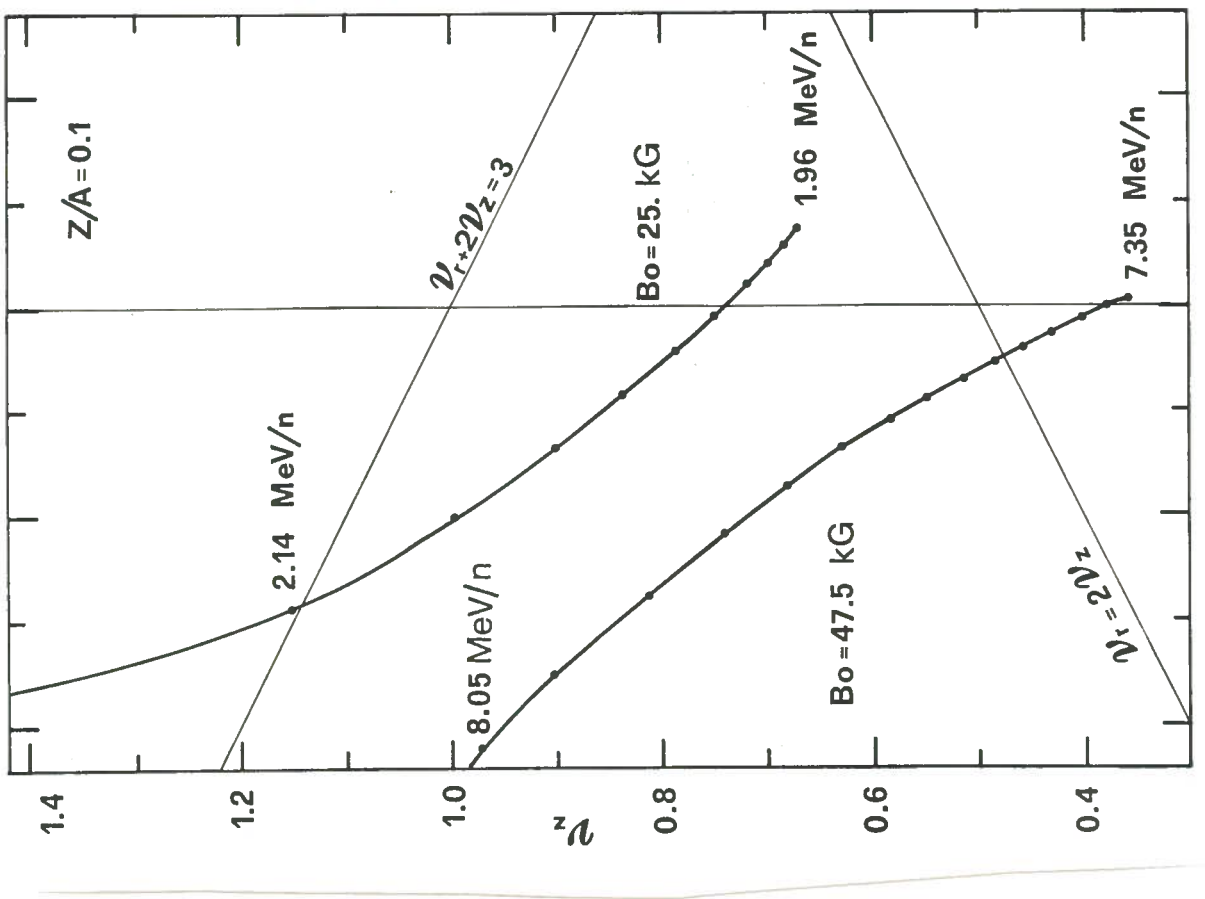

FIG. 12 - Operating (ν_r, ν_z) plots for the ion with Z/A = 0.1 at different field levels.

i) The $\nu_r + 2\nu_z = 3$ resonance, which cannot be crossed since it produces a very strong axial blow-up[7], sets in at progressively inner radii the lower the average field level. Physically this derives from the flutter increase proportional to $1/B^2$ at lower fields.

ii) As a consequence beam extraction must take place at progressively more internal radii.

iii) A further consequence is that the presence of the resonance effectively determines a lower field limit, below which the beam cannot be extracted. In our case this limit turns out to be approximately 22 kgauss.

4. - ACCELERATED BEAM STUDIES

4. 1. - Accelerated Orbits

All studies of accelerated orbits reported here use 360 deg maps obtained as described in Par. 2.

Everyone of the twelve ions has been accelerated starting from $\theta = 0$ deg and an initial energy per nucleon, T/A_I, corresponding to at least ten turns before the $\nu_r = 1$ resonance. The starting conditions for the central ray, i. e. the radius, R_I, the radial momentum, Pr_I, and the phase, Φ_I, with respect to the rf are given by the equilibrium orbit data and are listed in Table III, together with the axial, ε_z, and the radial, ε_x, emittance of the accelerated beam. The latter is around 5-7 mm mrad both in the axial and radial phase space. Each phase space is represented by eight particles whose initial con-

TABLE III - Starting conditions (θ = 0 deg) for the acceleration of the twelve ions studied.

Z/A	B_o (kG)	T/A_I (MeV/n)	R_I (cm)	Pr_I (cm)	Φ_r (deg)	ε_x (mm*mrad)	ε_z (mm*mrad)
0. 5	31. 3	93	84. 12	6. 00	- 39. 99	5. 4	5. 1
0. 5	26. 5	60	81. 64	8. 43	- 20. 96	5. 8	5. 8
0. 5	22	38	79. 39	11. 26	- 7. 76	6. 9	7. 1
0. 4	22	17	64. 93	8. 63	- 7. 27	7. 2	7. 1
0. 3	41. 4	55	83. 44	4. 71	- 34. 75	5. 1	5. 6
0. 3	22	10	67. 13	9. 53	- 5. 35	6. 4	7. 2
0. 25	45. 5	45	82. 89	4. 43	- 33. 10	5. 3	5. 0
0. 25	40	33. 5	82. 14	5. 29	- 25. 73	5. 4	5. 1
0. 25	38	30. 7	83. 10	5. 23	- 25. 69	6. 1	5. 3
0. 25	30	18. 3	82. 22	7. 10	- 12. 57	5. 9	5. 6
0. 1	47. 5	7. 3	82. 27	4. 39	- 17. 17	5. 2	5. 0
0. 1	25	1. 5	69. 76	9. 08	- 0. 94	6. 3	6. 2

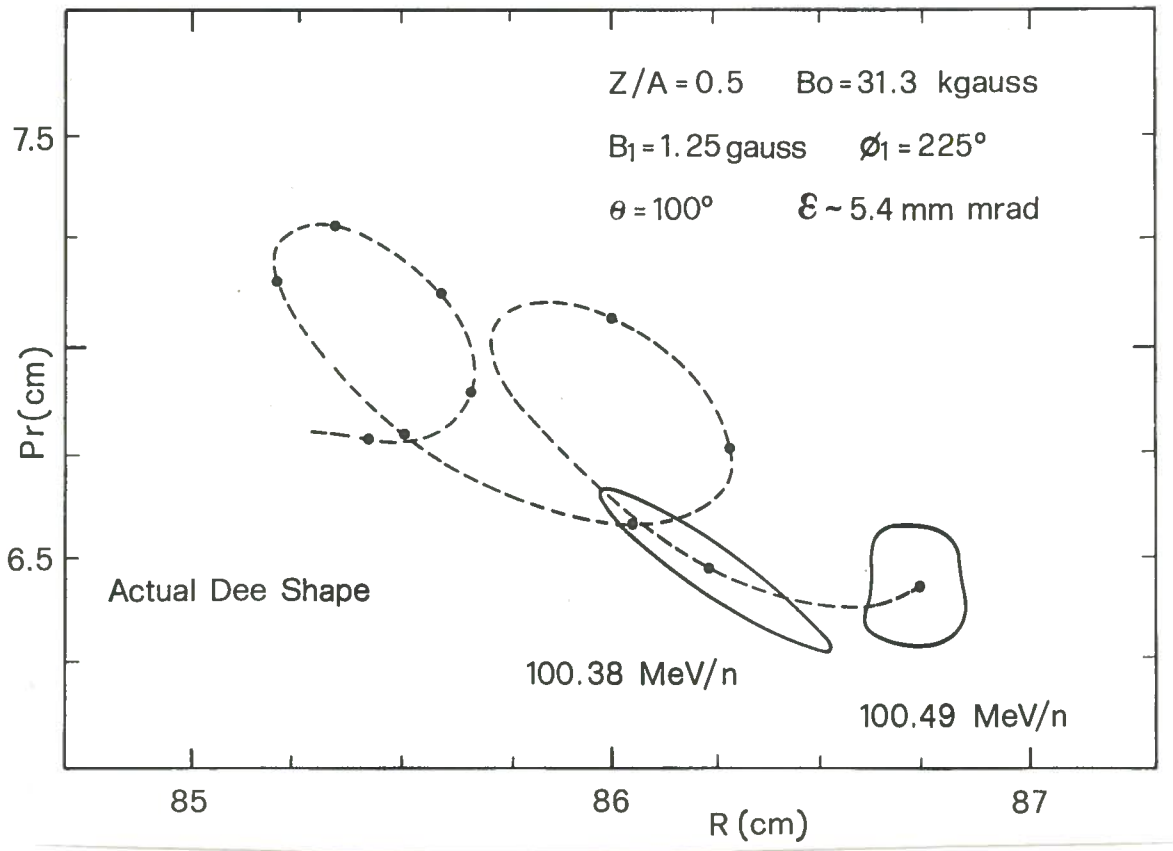

FIG. 30 - Radial phase space at extraction for the ion with Z/A = 0.5 and B_o = 31.3 kG accelerated with the actual dee shape.

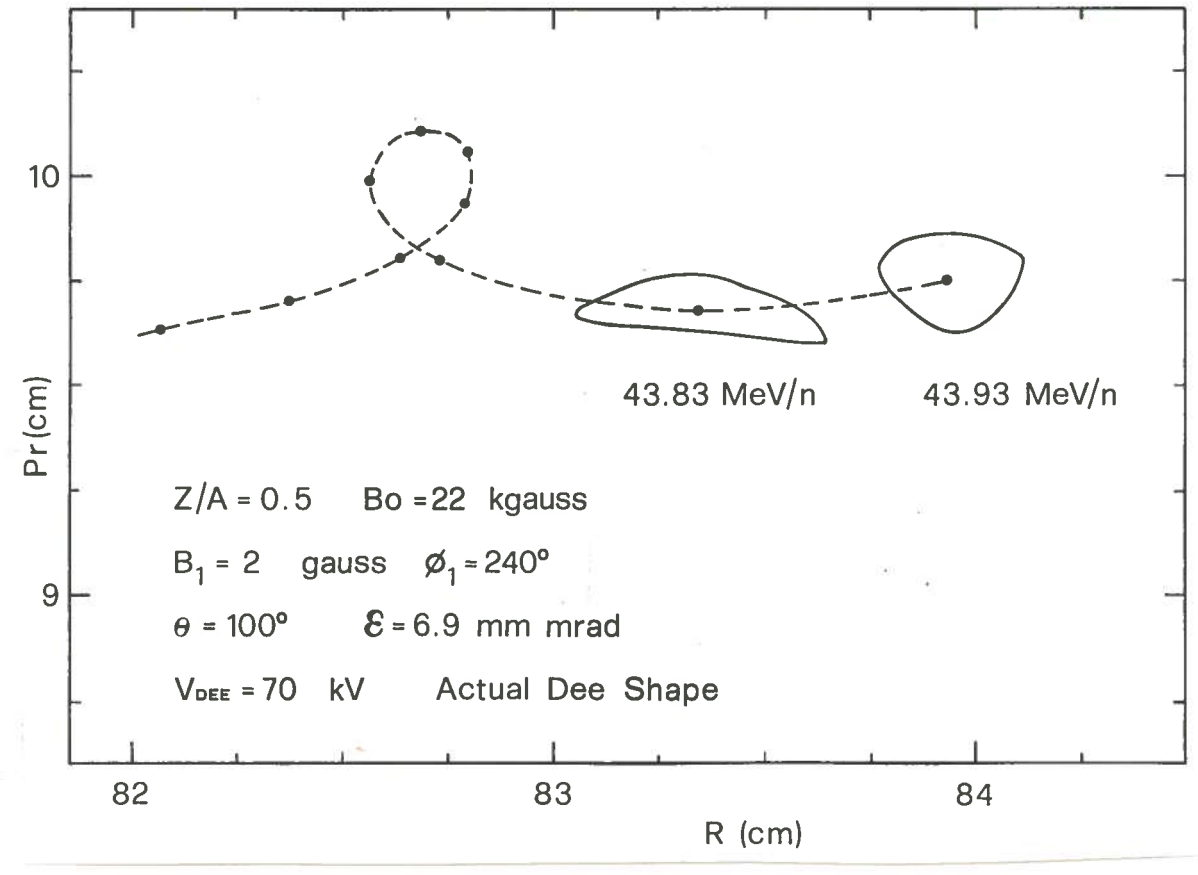

FIG. 31 - Radial phase space at extraction for the ion with Z/A = 0.5 and B_o = 22 kG accelerated with the actual dee shape.

TABLE IX - Acceleration parameters for the three ions accelerated with the actual shape dee.

Z/A	B_o (kG)	V (kV)	ν_{rf} (MHz)	h	B_1 (gauss)	Φ_1 (deg)
0.5	31.3	100	24.03	1	1.25	225
0.5	22	70	16.89	1	2	240
0.25	45.5	100	17.47	1	4	229

TABLE X - Beam condition at the extraction turn at $\theta = 100$ deg for the ions accelerated with the actual shape dee.

Z/A	B_o (kG)	R_F (cm)	Pr_F (cm)	Φ_F (deg)	T/A_F (MeV/n)	ΔR (mm)	z_{max} (mm)
0.5	31.3	86.74	6.43	46.98	100.49	0.7	2.6
0.5	22	83.94	9.76	9.20	43.97	2.2	4.8
0.25	45.5	86.70	4.38	29.34	49.33	1.4	5.8

The most critical ion is the one with $Z/A = 0.25$ and $B_o = 45.5$ kG, which exhibits a large axial dimension (5.8 mm) at the crossing of the $\nu_r = 2\nu_z$ resonance. By changing slightly the acceleration conditions it is possible to reduce the maximum axial displacement by 10%, but the beam to beam separation becomes much smaller and some distortions become evident. We have decided to choose the solution which allows a good radial phase space behaviour.

As a conclusion we can say that:

i) With a proper choice of the first harmonic amplitude and its phase, the beam to beam separation, as well as the phase space behaviour are comparable to those obtained with a continuous spiralling dee as presented in the previous paragraphs.

ii) The amplitudes of the required first harmonic component remain around a few gauss and therefore they can be easily provided by the 19th and the 20th trim coils.

Further tests will be made when data on the electric field in the region around R = 87 cm, where the dee shape changes, will be available.

5. - CONCLUSIONS

On the basis of the results presented here the following considerations can be outlined:

a) The twelve ions used in this study seem completely sufficient to describe the operating characteristics of the machine. In fact none of the ions in the middle of the operating diagram has shown behaviors markedly different from those on the borders.

b) The magnetic field used in beam dynamics studies must be the actual one in every detail. Any attempt to analyze beam dynamics features without accurate values of the isochronous field and its harmonics will give unreliable results.

c) The beam dynamics is indeed very critical near extraction. Therefore not only the magnetic field but also (see par. 4.3) the electric field used in the acceleration must be known with very high precision.

d) The centering of the beam is of paramount importance for the beam dynamics. The results presented here are valid only for centered beams. An investigation of off-centering effects is presently underway.

An important feature observed during this work (par. 3) is the shifting of the radial position at which a given ion crosses the resonances as a function of the field level. The "radial movement of the resonances" in the Milan superconducting cyclotron is larger than that of the MSU K=500 cyclotron[7]. This is due to the larger operating range, in terms of field level, of the Milan cyclotron.

This, while by no means jeopardizing the overall cyclotron performances, has some consequences on the operation of the machine, namely:

i) The radial span of the $\nu_r = 1$ resonance dictates the use of two trim coils to produce, at the proper radius, the first harmonic field component required to extract each ion.

ii) The $\nu_r + 2\nu_z = 3$ resonance (see par. 3.4.1) poses a limit on the lower magnetic field at which the ions can be successfully extracted. This limit seems to be 22 kG.

iii) As a consequence of the $\nu_r + 2\nu_z = 3$ resonance and of the limit of 140 kV/cm on the electric field in the deflector, any attempt to reduce the radial span of the deflectors below 3 cm has failed. The choice of a radially moveable extraction system is therefore mandatory.

iv) $^3He^{++}$ can be accelerated only in a very narrow range of energies (89-99 MeV/n). This indicates that the possibility of accelerating particles with higher Z/A values, such as protons, is, at best, remote.

This survey of beam dynamics shows, nevertheless, that no difficulties are expected in obtaining proper beams for the subsequent extraction, provided that the magnetic field is close to the one used here, both in terms of isochronism and harmonic content.

Since these results are deemed sufficiently consistent, no further analysis will be carried out until magnetic field measurements are available except the one, mentioned above, on the effect of centering errors.

REFERENCES

(1) - E. Fabrici and A. Salomone, The Extraction System for the Superconducting Cyclotron at the University of Milan, Proceedings of the 9th International Conference on Cyclotrons and their Applications, Caen 1981 (Les Editions de Physique, 1982), pag. 501.

(2) - E. Acerbi et al., The Milan Superconducting Cyclotron Project, Proceedings of the 9th International Conference on Cyclotrons and their Applications, Caen 1981 (Les Editions de Physique, 1982), pag. 169.

(3) - E. Fabrici and A. Salomone, The Extraction System for the Milan Superconducting Cyclotron, to be published.

(4) - G. Bellomo and L. Serafini, Design of the Magnetic Field for the Milan Superconducting Cyclotron, to be published.

(5) - R. F. Holsinger and C. Iselin, POISCR, The CERN POISSION Program Package, CERN Internal Report.

(6) - M. M. Gordon, Nuclear Instr. and Meth. 169, 327 (1980).

(7) - E. Fabrici, D. Johnson and F. Resmini, Nuclear Instr. and Meth. 180, 319 (1981).

APPENDIX A

Beam envelopes before extraction as a function of the azimuth for the eight ions on the border of the operating plot.

TH	.5/31.3	.5/22.	.4/22.	.3/414	.3/22.	.25/55.5	.1/47.5	.1/25.
104	86.71264	84.09628	84.53670	86.46545	83.23207	86.75026	85.93847	83.55962
106	86.92794	84.45697	84.90619	86.64019	83.60914	86.91551	86.10986	83.89797
108	87.14401	84.81954	85.27453	86.81526	83.99497	87.07636	86.27832	84.24314
110	87.34953	85.17492	85.63295	86.98292	84.37823	87.23018	86.44076	84.58468
112	87.54163	85.51532	85.97412	87.14087	84.74988	87.37507	86.59476	84.91469
114	87.71827	85.83475	86.29267	87.28745	85.10237	87.50959	86.73851	85.22649
116	87.87811	86.12900	86.58494	87.42143	85.43021	87.63272	86.87066	85.51521
118	88.02018	86.39519	86.84848	87.54191	85.73016	87.74369	86.99023	85.77758
120	88.14383	86.63140	87.08167	87.64821	86.00084	87.84193	87.09650	86.01137
122	88.25176	86.83628	87.28344	87.73986	86.23876	87.92700	87.18890	86.21505
124	88.34308	87.00893	87.45309	87.81645	86.44272	87.99860	87.26898	86.38759
126	88.41505	87.14873	87.59016	87.87771	86.61187	88.05645	87.33591	86.52825
128	88.46750	87.25739	87.69431	87.92340	86.74565	88.10036	87.38798	86.63652
130	88.50030	87.33373	87.76530	87.95331	86.84361	88.13016	87.42500	86.71205
132	88.51334	87.37614	87.80289	87.96730	86.90541	88.14571	87.44679	86.75454
134	88.50649	87.38437	87.80687	87.96522	86.93079	88.14688	87.45321	86.76377
136	88.47964	87.35814	87.77696	87.94692	86.91945	88.13355	87.44413	86.73955
138	88.43263	87.29716	87.71285	87.91227	86.87113	88.10561	87.41943	86.68169
140	88.36532	87.20112	87.61418	87.86114	86.78554	88.06292	87.37901	86.58999
142	88.27752	87.06968	87.48054	87.79340	86.66235	88.00538	87.32274	86.46798
144	88.16905	86.90756	87.31274	87.70891	86.50128	87.93287	87.25055	86.31239
146	88.03973	86.71090	87.11502	87.60758	86.30206	87.84529	87.16236	86.12250
148	87.88946	86.47804	86.88124	87.48938	86.06460	87.74261	87.05816	85.89834
150	87.71855	86.20934	86.61165	87.35455	85.78934	87.62505	86.93821	85.64047
152	87.52860	85.90688	86.30834	87.20429	85.47834	87.49372	86.80362	85.35101
154	87.32411	85.57659	85.97761	87.04220	85.13733	87.35196	86.65919	85.03525
156	87.11206	85.22768	85.62924	86.87398	84.77526	87.20476	86.50937	84.70147
158	86.89851	84.86921	85.27245	86.70688	84.40130	87.05637	86.35751	84.35803
160	86.68778	84.50863	84.91453	86.54143	84.02332	86.90972	86.20683	84.01443

TH	.5/31.3	.5/22.	.4/22.	.3/414	.3/22.	.25/55.5	.1/47.5	.1/25.
162	86.48570	84.15185	84.56114	86.38006	83.64775	86.76695	86.05966	83.67668
164	86.29115	83.80351	84.21670	86.22474	83.27978	86.62955	85.92138	83.34657
166	86.10587	83.46799	83.88797	86.07646	82.92350	86.49849	85.78991	83.02788
168	85.93114	83.14864	83.57575	85.93621	82.58914	86.37461	85.66586	82.72867
170	85.76796	82.84745	83.28082	85.80476	82.27647	86.25856	85.54995	82.44576
172	85.61714	82.56838	83.00489	85.68274	81.98312	86.15087	85.44275	82.18082
174	85.47932	82.30972	82.74932	85.57063	81.71060	86.05195	85.34471	81.93519
176	85.35501	82.07256	82.51515	85.46882	81.46011	85.96213	85.25618	81.70991
178	85.24463	81.85777	82.30326	85.37764	81.23259	85.88169	85.17744	81.50577
180	85.14851	81.66606	82.11433	85.29734	81.02879	85.81084	85.10872	81.32342
182	85.06692	81.49799	81.94890	85.22895	80.84933	85.74977	85.05021	81.16334
184	85.00006	81.35402	81.80742	85.17587	80.69469	85.69865	85.00206	81.02594
186	84.94898	81.23453	81.69027	85.13422	80.56527	85.65758	84.96441	80.91149
188	84.91450	81.13981	81.59774	85.10411	80.46138	85.62669	84.93735	80.82025
190	84.89511	81.07012	81.53007	85.08564	80.38330	85.60605	84.92097	80.75238
192	84.89088	81.02566	81.48746	85.07889	80.33123	85.59573	84.91533	80.70802
194	84.90184	81.00662	81.47009	85.08391	80.30538	85.59580	84.92048	80.68728
196	84.92798	81.01313	81.47811	85.10298	80.30591	85.60630	84.93648	80.69023
198	84.96929	81.04535	81.51164	85.13498	80.33297	85.62726	84.96336	80.71695
200	85.02576	81.10338	81.57081	85.17892	80.38670	85.65871	85.00113	80.76749
202	85.09733	81.18734	81.65573	85.23480	80.46723	85.70067	85.04982	80.84190
204	85.18396	81.29734	81.76649	85.30262	80.57469	85.75316	85.10945	80.94023
206	85.28558	81.43346	81.90319	85.38238	80.70922	85.81617	85.18002	81.06254
208	85.40210	81.59580	82.06590	85.47406	80.87092	85.88972	85.26153	81.20885
210	85.53343	81.78442	82.25469	85.57763	81.05992	85.97379	85.35398	81.37921
212	85.67944	81.99937	82.46957	85.69305	81.27628	86.06835	85.45733	81.57434
214	85.83995	82.24061	82.71052	85.82023	81.52005	86.17335	85.57154	81.79475
216	86.01471	82.50801	82.97737	85.95901	81.79116	86.28865	85.69648	82.03906
218	86.20316	82.80457	83.26964	86.10904	82.08928	86.41395	85.83186	82.30692
220	86.40402	83.12678	83.58615	86.26942	82.41355	86.54842	85.97689	82.59745
222	86.61430	83.47121	83.92420	86.43809	82.76202	86.69032	86.12967	82.90875
224	86.82910	83.83342	84.27874	86.61179	83.13098	86.83636	86.28978	83.23740
226	87.04195	84.20754	84.64469	86.78484	83.51563	86.98137	86.45002	83.57983
228	87.24805	84.58513	85.01160	86.95326	83.90997	87.13442	86.60659	83.93144
230	87.44421	84.95686	85.37024	87.11411	84.30253	87.28452	86.75662	84.28150
232	87.62872	85.31454	85.71292	87.26521	84.68414	87.42574	86.89791	84.62196
234	87.79785	85.65178	86.03389	87.40495	85.04712	87.55668	87.02883	84.94574
236	87.95084	85.96405	86.32913	87.53218	85.38586	87.67633	87.14817	85.24754
238	88.08911	86.24828	86.59597	87.64602	85.69647	87.78393	87.25634	85.52378
240	88.20920	86.50237	86.83258	87.74583	85.97633	87.87894	87.35287	85.77200

TH	.5/31.3	.5/22.	.4/22.	.3/414	.3/22.	.25/55.5	.1/47.5	.1/25.
242	88.31068	86.72493	87.03920	87.83114	86.22366	87.96091	87.43578	85.99053
244	88.39322	86.91500	87.21577	87.90158	86.43726	88.02954	87.50468	86.17823
246	88.45660	87.07191	87.35955	87.95686	86.61629	88.08457	87.55927	86.33429
248	88.50063	87.19523	87.47015	87.99674	86.76018	88.12579	87.59932	86.45817
250	88.52518	87.28461	87.54731	88.02104	86.86851	88.15305	87.62462	86.54947
252	88.53011	87.33980	87.59076	88.02960	86.94096	88.16620	87.63502	86.60790
254	88.51530	87.36055	87.60028	88.02227	86.97728	88.16510	87.63037	86.63324
256	88.48061	87.34662	87.57561	87.99890	86.97721	88.14966	87.61054	86.62530
258	88.42589	87.29776	87.51648	87.95937	86.94052	88.11974	87.57541	86.58393
260	88.35100	87.21370	87.42257	87.90356	86.86695	88.07524	87.52488	86.50898
262	88.25581	87.09421	87.29361	87.83136	86.75726	88.01609	87.45886	86.40035
264	88.14030	86.93916	87.12942	87.74279	86.61224	87.94232	87.37740	86.25805
266	88.00487	86.74874	86.93021	87.63814	86.43015	87.85429	87.28076	86.08229
268	87.84996	86.52320	86.69622	87.51851	86.21124	87.75243	87.16932	85.87339
270	87.67591	86.26720	86.42779	87.38609	85.95602	87.63701	87.04337	85.63194
272	87.48822	85.97889	86.12683	87.23935	85.66644	87.50902	86.90394	85.35997
274	87.28702	85.66377	85.79917	87.08170	85.34813	87.37156	86.75405	85.06493
276	87.07888	85.33075	85.45396	86.91822	85.00997	87.22925	86.59834	84.75391
278	86.86959	84.98865	85.10009	86.75339	84.66099	87.08608	86.44103	84.43370
280	86.66329	84.64472	84.74482	86.59055	84.30888	86.94502	86.28534	84.11119
282	86.46290	84.30678	84.39388	86.43215	83.95980	86.80821	86.13363	83.79201
284	86.27032	83.97817	84.05178	86.27999	83.61871	86.67705	85.99139	83.48069
286	86.08728	83.66253	83.72466	86.13506	83.29100	86.55245	85.85602	83.18162
288	85.91526	83.36258	83.41463	85.99821	82.98747	86.43509	85.72818	82.90176
290	85.75744	83.07966	83.12201	85.87258	82.70123	86.32555	85.60854	82.63820
292	85.61200	82.81550	82.84887	85.75920	82.43411	86.22432	85.49861	82.39261
294	85.47958	82.57147	82.59892	85.65566	82.18754	86.13181	85.39876	82.16627
296	85.36070	82.34864	82.37053	85.56236	81.96268	86.04835	85.30846	81.96018
298	85.25577	82.14788	82.16457	85.47961	81.76041	85.97421	85.22800	81.77513
300	85.16512	81.96988	81.98173	85.40766	81.58146	85.90962	85.15762	81.61175
302	85.08903	81.81520	81.82258	85.34674	81.42640	85.85475	85.09751	81.47050
304	85.02770	81.68428	81.68756	85.29701	81.29569	85.80975	85.04784	81.35176
306	84.98128	81.57750	81.57703	85.25861	81.19244	85.77474	85.00872	81.25581
308	84.94990	81.49514	81.49129	85.23166	81.11592	85.74983	84.98027	81.18287
310	84.93362	81.43745	81.43059	85.21830	81.06467	85.73508	84.96256	81.13311
312	84.93251	81.40463	81.39512	85.21697	81.03887	85.73057	84.95567	81.10665
314	84.94658	81.39685	81.38506	85.22731	81.03870	85.73634	84.95966	81.10358
316	84.97583	81.41425	81.40055	85.24933	81.06431	85.75243	94.97456	81.12397
318	85.02027	81.45696	81.44172	85.28309	81.11583	85.77887	85.00041	81.16789
320	85.07984	81.52509	81.50868	85.32858	81.19338	85.81568	85.03725	81.23536

TH	.5/31.3	.5/22.	.4/22.	.3/414	.3/22.	.25/55.5	.1/47.5	.1/25.
322	85.15451	81.61874	81.60155	85.38582	81.29707	85.86288	85.08508	81.32644
324	85.24422	81.73800	81.72042	85.45481	81.42701	85.92047	85.14393	81.44115
326	85.34889	81.88295	81.86622	85.53554	81.58328	85.98845	85.21380	81.57952
328	85.46844	82.05366	82.03930	85.62800	81.76598	86.06681	85.29470	81.74157
330	85.60277	82.25016	82.23859	85.73391	81.97518	86.15554	85.38661	81.92930
332	85.75175	82.47248	82.46412	85.85182	82.21090	86.25461	85.48952	82.14119
334	85.91597	82.72056	82.71583	85.98135	82.47312	86.36394	85.60337	82.37669
336	86.09571	82.99421	82.99356	86.12233	82.76168	86.48341	85.72804	82.63561
338	86.28911	83.29296	83.29683	86.27441	83.07612	86.61269	85.86323	82.91754
340	86.49485	83.61560	83.62442	86.43666	83.41529	86.75095	86.00817	83.22143
342	86.70997	83.95944	83.97360	86.60711	83.77653	86.89655	86.16093	83.54500
344	86.92939	84.31942	84.33922	86.78224	84.15484	87.04588	86.32112	83.88411
346	87.14667	84.68940	84.71616	86.95638	84.54552	87.19384	86.48146	84.23588
348	87.35707	85.05983	85.09369	87.12563	84.93787	87.33698	86.63822	84.59206
350	87.55678	85.42185	85.46264	87.28718	85.32203	87.47290	86.78942	84.94309
352	87.74312	85.76797	85.81545	87.43898	85.68998	87.59985	86.93299	85.28131
354	87.91427	86.09257	86.14644	87.57951	86.03572	87.71655	87.06637	85.60053
356	88.06953	86.39175	86.45172	87.70768	86.35509	87.82203	87.18837	85.89638
358	88.21132	86.66289	86.72869	87.82267	86.64533	87.91557	87.29810	86.16594
0	88.33526	86.90425	86.97562	87.92389	86.90463	87.99665	87.39492	86.40727
2	88.44094	87.11467	87.19135	88.01090	87.13179	88.06485	87.47833	86.61908
4	88.52809	87.29338	87.37517	88.08334	87.32605	88.12074	87.54795	86.80050
6	88.59647	87.43983	87.52659	88.14096	87.48695	88.18290	87.60347	86.95092
8	88.64593	87.55365	87.64528	88.18352	87.61416	88.23150	87.64466	87.06995
10	88.67632	87.63455	87.73103	88.21084	87.70746	88.26637	87.67130	87.15730
12	88.68753	87.68229	87.78362	88.22277	87.76668	88.28738	87.68325	87.21277
14	88.67944	87.69666	87.80288	88.21916	87.79163	88.29440	87.68035	87.23619
16	88.65192	87.67741	87.78857	88.19988	87.78211	88.28733	87.66247	87.22740
18	88.60485	87.62428	87.74045	88.16480	87.73787	88.26606	87.62949	87.18624
20	88.53806	87.53695	87.65819	88.11377	87.65859	88.23048	87.58129	87.11252
22	88.45137	87.41507	87.54144	88.04667	87.54390	88.18048	87.51777	87.00603
24	88.34458	87.26183	87.38978	87.96335	87.39340	88.11593	87.43880	86.86656
26	88.21748	87.07427	87.20282	87.86369	87.20677	88.03675	87.34430	86.69390
28	88.06997	86.85428	86.98029	87.74811	86.98574	87.94289	87.23425	86.48802
30	87.90601	86.60338	86.72266	87.61916	86.72843	87.83455	87.10889	86.24938
32	87.72373	86.31930	86.43396	87.47523	86.43691	87.71284	86.96931	85.98016
34	87.52730	86.00829	86.11836	87.31991	86.11767	87.58107	86.81876	85.68606
36	87.32365	85.67999	85.78572	87.15861	85.78072	87.44422	86.66216	85.37764
38	87.11870	85.34350	85.44523	86.99590	85.43540	87.30636	86.50386	85.06202
40	86.91636	85.00596	85.10408	86.83492	85.08899	87.17028	86.34698	84.74567
42	86.71918	84.67293	84.76776	86.67791	84.74708	87.03782	86.19378	84.43382

TH	.5/31.3	.5/22.	.4/22.	.3/414	.3/22.	.25/55.5	.1/47.5	.1/25.
44	86.52912	84.34868	84.44057	86.52652	84.41402	86.91039	86.04978	84.13054
46	86.34858	84.03806	84.12987	86.38198	84.09885	86.78911	85.91235	83.84287
48	86.18076	83.74257	83.83478	86.24525	83.79950	86.67479	85.78242	83.57154
50	86.02420	83.46393	83.55685	86.11707	83.51720	86.56805	85.66072	83.31643
52	85.87970	83.20382	83.29773	86.00198	83.25364	86.46940	85.54783	83.07907
54	85.74788	82.96356	83.05872	85.89773	83.01014	86.37924	85.44467	82.86063
56	85.62926	82.74419	82.84089	85.80350	82.78779	86.29790	85.35368	82.66204
58	85.52426	82.54850	82.64507	85.71959	82.58743	86.22564	85.27260	82.48403
60	85.43319	82.37542	82.47194	85.64627	82.40974	86.16268	85.20166	82.32719
62	85.35633	82.22529	82.32202	85.58375	82.25527	86.10919	85.14107	82.19197
64	85.29389	82.09855	82.19577	85.53220	82.12447	86.06533	85.09097	82.07872
66	85.24601	81.99556	82.09353	85.49176	82.01770	86.03121	85.05150	81.98771
68	85.21284	81.91662	82.01560	85.46256	81.93526	86.00693	85.02277	81.91916
70	85.19444	81.86197	81.96222	85.44469	81.87739	85.99258	85.00487	81.87321
72	85.19090	81.83181	81.93359	85.43999	81.84430	85.98823	84.99788	81.85001
74	85.20226	81.82632	81.93184	85.44748	81.83617	85.99395	85.00187	81.84963
76	85.22857	81.84565	81.95731	85.46654	81.85316	86.00981	85.01692	81.87216
78	85.26989	81.88995	82.00800	85.49726	81.89541	86.03591	85.04310	81.91766
80	85.32629	81.95933	82.08403	85.53977	81.96306	86.07237	85.08052	81.98618
82	85.39783	82.05391	82.18550	85.59415	82.05622	86.11931	85.12924	82.07776
84	85.48453	82.17378	82.31250	85.66047	82.17500	86.17678	85.18934	82.19423
86	85.58631	82.31902	82.46510	85.73873	82.31948	86.24480	85.26082	82.33475
88	85.70305	82.48965	82.64335	85.82886	82.48971	86.32330	85.34365	82.49835
90	85.83455	82.68568	82.84724	85.93076	82.68572	86.41218	85.43776	82.68498
92	85.98056	82.90709	83.07674	86.04428	82.90750	86.51129	85.54305	82.89458
94	86.14268	83.15376	83.33173	86.16926	83.15495	86.62049	85.65941	83.12703
96	86.31897	83.42545	83.61195	86.30551	83.42785	86.73960	85.78669	83.38206
98	86.50862	83.72157	83.91679	86.45263	83.72561	86.86828	85.92457	83.65917
100	86.71026	84.04080	84.24485	86.60970	84.04690	87.00565	86.07225	83.95711
102	86.92100	84.38015	84.59296	86.77479	84.38864	87.15026	86.22787	84.27310

APPENDIX B

Maximum radius of the envelopes in appendix A as a function of the azimuth.

TH(DEG)	R(CM)	TH(DEG)	R(CM)	TH(DEG)	R(CM)	TH(DEG)	R(CM)
104	86.75030	194	85.59580	284	86.67700	14	88.69200
106	86.92670	196	85.60630	286	86.55250	16	88.66300
108	87.14610	198	85.62730	288	86.43510	18	88.61450
110	87.35510	200	85.65870	290	86.32560	20	88.54620
112	87.55070	202	85.70070	292	86.22430	22	88.45810
114	87.73100	204	85.75320	294	86.13180	24	88.34990
116	87.89450	206	85.81620	296	86.04840	26	88.22140
118	88.04030	208	85.88970	298	85.97420	28	88.07240
120	88.16790	210	85.97380	300	85.90960	30	87.90440
122	88.27660	212	86.06830	302	85.85470	32	87.72060
124	88.36630	214	86.17340	304	85.80970	34	87.58110
126	88.43670	216	86.28860	306	85.77470	36	87.44420
128	88.48760	218	86.41390	308	85.74980	38	87.30640
130	88.51890	220	86.54840	310	85.73510	40	87.17030
132	88.53040	222	86.69030	312	85.73060	42	87.03780
134	88.52220	224	86.84060	314	85.73630	44	86.91040
136	88.49390	226	87.05740	316	85.75240	46	86.78910
138	88.44550	228	87.26740	318	85.77890	48	86.67480
140	88.37690	230	87.46690	320	85.81570	50	86.56810
142	88.28770	232	87.65290	322	85.86290	52	86.46940
144	88.17800	234	87.82360	324	85.92050	54	86.37920
146	88.04730	236	87.97770	326	85.98850	56	86.29790
148	87.89580	238	88.11420	328	86.06680	58	86.22560
150	87.72360	240	88.23270	330	86.15550	60	86.16270
152	87.53240	242	88.33250	332	86.25460	62	86.10920
154	87.35200	244	88.41340	334	86.36390	64	86.06530
156	87.20480	246	88.47530	336	86.48340	66	86.03120
158	87.05640	248	88.51780	338	86.61270	68	86.00690
160	86.90970	250	88.54080	340	86.75090	70	85.99260

TH(DEG)	R(CM)	TH(DEG)	R(CM)	TH(DEG)	R(CM)	TH(DEG)	R(CM)
162	86.76690	252	88.54430	342	86.89660	72	85.98820
164	86.62950	254	88.52800	344	87.04590	74	85.99390
166	86.49850	256	88.49190	346	87.19380	76	86.00980
168	86.37460	258	88.43580	348	87.37540	78	86.03590
170	86.25860	260	88.35960	350	87.57750	80	86.07240
172	86.15090	262	88.26300	352	87.76620	82	86.11930
174	86.05200	264	88.14620	354	87.93980	84	86.17680
176	85.96210	266	88.00940	356	88.09700	86	86.24480
178	85.88170	268	87.85320	358	88.23700	88	86.32330
180	85.81080	270	87.67780	0	88.35920	90	86.41220
182	85.74980	272	87.50900	2	88.46320	92	86.51130
184	85.69870	274	87.37160	4	88.54860	94	86.62050
186	85.65760	276	87.22920	6	88.61530	96	86.73960
188	85.62670	278	87.08610	8	88.66320	98	86.86830
190	85.60600	280	86.94500	10	88.69200	100	87.00560
192	85.59570	282	86.80820	12	88.70160	102	87.15030